

Modeling the Dynamic Behavior of Personal Watercrafts

Tianhao Ren

21772005

School of Mechanical and Chemical Engineering

University of Western Australia

Supervisor: Thomas Bräunl

School of Electrical, Electronic and Computer Engineering

University of Western Australia

Final Year Project Thesis

School of Mechanical and Chemical Engineering

University of Western Australia

Word count: 6424

Date of Submission: 28th June 2018

ABSTRACT

Under the Renewable Energy Vehicle Project (REV Project), the aim for the REVski project is to convert a traditional petrol-based jet ski to an electrically powered jet ski. Currently, the first prototype of the electric jet ski is completed, and several on-water field tests have been conducted. However, the electric Jet ski (REVski) is yet to have the competitive performance to its traditional counterpart.

Based on the current model of the electric Jet-ski, this thesis focuses on the establishment and computation of small personal watercraft's maneuvering motion model. Firstly, a complete 6-DOF dynamic model of the Jet-ski is established using commercial CFD software STAR-CCM+. Secondly, a 3-DOF mathematical maneuvering model for general small personal watercraft is developed based on the linear regression approximation of the hydrodynamic coefficients. Finally, the mathematical model is simulated using MATLAB and results were compared and analyzed.

In the case of hydrodynamic calculation, the method of planar motion mechanism test is used. Firstly, the correctness of the calculation method is verified through the simple geometry of additional mass computation. Then 8 hydrodynamic coefficients related to maneuvering the "REVski" with 3 DOF under hydrodynamic condition.

In order to simulate the behavior of general small personal watercraft, the method of linear approximation of hydrodynamic coefficients is used. In this way, calculating the hydrodynamic coefficients of a certain small personal watercraft does not require full detail of geometry anymore. The simplified hydrodynamic formulas using linear approximation is used to build up a MATLAB model, and the results are compared with CFD model and actual field test data.

Acknowledgments

I would like to begin by thanking my supervisor, Professor Thomas Bräunl , for his continuous guidance and support throughout my final year project. None would be achieved without his insightful guidance.

I would also like to thank Mark Henderson and his team in the Mechanical Workshop for his practical advises and reliable workmanship.

I would like to express my gratitude to my final year project teammates: Alexander Morgan, Maximilian Jacob and Hjariz Jahis. They help me out of many desperate times.

Finally, I would like to thank my ex-girlfriend, Jiayu Ding. I would like to thank her for breaking up with me so that I can have enough time to study my thesis and write the final essay.

content

1 Introduction.....	1
1.1 Project Background.....	1
1.3 Main content of this paper.....	2
2 Literature Review.....	3
2.1 Research Status on the Mathematical model of ship maneuvering.....	3
2.2 Research Status on Calculating hydrodynamic coefficients.....	4
2.3 Coordinate System.....	6
2.4 Definition of 6-DOF (degree of freedom) motion.....	6
2.5 Equation of translational movement.....	7
2.6 Equation of Rotary Movement.....	9
2.7 Forces Summary.....	10
3 Mathematical Model.....	11
3.1 Assumptions.....	11
3.2 Factors affecting Hydrodynamics.....	11
3.3 Taylor expansion of the hydrodynamic function.....	13
3.4 Linearization of the mathematical model.....	14
3.5 Computation of the Hydrodynamic coefficients.....	16
3.6 Operating Response Characteristics Equation.....	16
4 CFD simulation.....	18
4.1 Components Modeling.....	18
4.2 Hull Modeling.....	19
4.3 Thrusting System.....	21
4.4 Software Setup.....	23
4.5 Boundary Condition and other settings.....	24
4 MATLAB Simulation.....	25
4.1 MATLAB flow chart.....	25
4.2 SIMULINK layout.....	26
4.3 Inputs for The MATLAB Simulation.....	28
4.4 Settings for the solver.....	29
5 Result and Discussion.....	30
5.1 Drag acceleration simulation.....	30
5.2 Bobbing Issue.....	33
5.3 Comparison of Hydrodynamic Coefficients.....	34
6 Conclusion.....	37
7 Future Work.....	38
8 Reference.....	39
9 Appendix.....	41

1 Introduction

1.1 Project Background

The first Jet Ski was invented by Kawasaki motors in 1972[1]. Since then, personal watercrafts have been widely used for leisure activities. With all current personal watercrafts being powered by a powerful petrol engine, personal watercrafts always come with severe tailpipe emission and noise pollution issues. As a result, regulations and restrictions for operating personal watercrafts have been made in America and Europe.

To solve this issue, under the Renewable Energy Vehicle Project (REV Project), the REVSki project aims to convert a traditional petrol-based Jet Ski to an Electric Jet Ski. The idea of this project is to “have all the fun on water without noise and pollution.” The project is based on a second-hand Sea-Doo GTI 130, with its engine replaced with 50kW 3-phase AC induction motor and Lithium-iron Phosphate batteries system implemented inside the hull as shown in Figure.1. The REVSki is now capable of running 30 minutes and can hit a top speed of 31 KPH as is shown in Figure.2.



Figure.1 Sea-Doo GTI 130



Figure.2 REVski hitting Top speed of 31 KPH

1.3 Main content of this paper

The paper focuses on modeling the dynamic behavior of personal watercraft. The following 3 aspects will be emphasized:

1. The mathematical model of the ship motion
2. Simulation and hydrodynamic coefficient calculations based on STAR-CCM+
3. Simulation for general personal watercraft based on MATLAB

Firstly, a mathematical model for describing the behavior of personal watercraft is built. Secondly, A commercial CFD software called STAR-CCM+ is used for simulating the behavior of the REVski and calculating its hydrodynamic coefficients. Lastly, a simulation on MATLAB is developed based on the mathematical model for describing general personal watercraft.

The verification and validation of the CFD model and MATLAB model are carried out by comparing the results with actual field test recorded data. Given the fact that the REVski is the only object the author currently has access to, the MATLAB simulation is verified and validated by given the geometry parameters of the REVski.

2 Literature Review

2.1 Research Status on the Mathematical model of ship maneuvering

Being the most fundamental and critical part of all motion simulating and modeling problems, the first complete mathematical model for describing the behavior of ships, is introduced by K.S.M Davidson and L.I Schiff in late 1940s[2]. After decades of improvements and developments, there are mainly two kinds of a mathematical model that is used widely nowadays: the first model is developed by American scholar Abkowitz in 1964. The method is called integral hydrodynamic model, which is based on the Taylor series expansion of hydrodynamic force (torque) in the equation of motion[3]. In 1980, several modifications and improvements were made for describing the effects of the propeller of impeller and rudder[4].

The main idea of the integral hydrodynamic model is to treat the hull, impeller, and the rudder as one integrated part, which means the hydrodynamic forces applied to it can be modeled as a function of the flow field properties, hull geometry and the kinematic state of the ship at each time interval. After properly modeled the force acting on the boat, the expression of force is. Therefore, Taylor expanded. Every term higher than third order is regarded as a hydrodynamic coefficient. There are several ways of determining those hydrodynamic coefficients. The one this paper adopted will be explained later. The advantages of the Integral hydrodynamic model are that firstly, the mathematical derivation is rigorous and, secondly, interferences between the hull, impeller and the rudder can be ignored[5]. Thirdly, the accuracy of the model can be controlled by adopting different methods of calculating the hydrodynamic coefficients.

Another popular model that is widely used is called the Separate Hydrodynamic Model developed by the MMG (Mathematical Modeling Group) in the 1970s[6]. the mean idea of the separate Hydrodynamic Model is to describe the performance of the rudder, hull, and impeller separately

rather than treating as a whole[7]. In such way, the calculated hydrodynamic forces are more accurate, and the interferences between each main component can be expressed and analyzed.

Apart from those two main mathematical model, there is another one called the first order linear corresponding model, also known as the Nomoto model[8]. This method treats the ship as a “plant,” treats rudder angle propeller forces as “inputs” then the dynamic behavior of the ship is the “output.” This model is often more practical when designing auto-piloting ship[9].

Up to date, all those mathematical model theories have been driven to maturity stage. Researchers have now begun to study on modeling more complicated situations such as dual-jet ship and extreme sea conditions[10].

2.2 Research Status on Calculating hydrodynamic coefficients

When adopting the Integral Hydrodynamic model, the most important aspect is to calculate the hydrodynamic coefficients of the certain object. Currently, there are basically three ways of calculating hydrodynamic coefficients:

The first method is called the constrained-structure testing method. In this method, firstly a physical model that is scaled down based on the object is built. Secondly, the model is put into the pool, and then the displacements are recorded when given a certain controlled exciting force. Lastly, the displacements and exciting forces together are used to calculate the hydrodynamic coefficients[11]. Theoretically, this method is the most reliable one. However, a lot of experiments are needed, and the accuracy of the hydrodynamic coefficients largely depends on the accuracy of the displacements and exciting forces. Moreover, deviations have been noticed on the field when using this method for calculating mass related hydrodynamic coefficients probably due to the “scale down” step.

Unlike the constrained-structure testing method that is mentioned above, the second method, free running testing method[12], doesn't require the "scale down" step. The hydrodynamic coefficients, in this method, is calculated by system discrimination when the input parameters (RPM of the impeller, rudder angle) and the output of the system (speed, turning angle) are recorded. In this way, errors generated in the "scale down" step can be eliminated. However, inevitably this method depends on the actual ship to complete several tests, which can be time-consuming and costly if the object is too big[12].

During the 1930s, thanks to the booming development of shipping industry and the demand from international trading, traditional ways of determining hydrodynamic coefficients gradually declined[13]. People started to study the numerical ways of determining hydrodynamic coefficients. Generally speaking, the numerical method for calculating hydrodynamic coefficients is achieved by firstly, mathematical modeling the ship geometry and the drainage, secondly, solving the specific control equation by given boundary conditions. However, this method took much longer time than the traditional method and had even lower accuracy until computer replaced hand-calculating in the late 1960s[14].

After that, the Numerical method for calculating hydrodynamic coefficients becomes even simpler thanks to the development of programming language. In 1997, Bailey, etc. developed a unified mathematical model which contains 6 degrees of freedom and a linear relationship between hydrodynamic coefficients and oscillation coefficients when encountering a sudden change of driving frequency[15]. Nowadays, scholars concentrate more on the collision hydrodynamic calculation or oil platform jacket hydrodynamic calculations[16].

2.3 Coordinate System

Before the mathematical model is developed, a suitable coordinate system needs to be determined ahead of everything. In this paper, an earth-fixed inertial coordinate $E - \zeta\eta\xi$, and a body fixed attached coordinate $O - xyz$ is chosen to describe the behavior of the ship as shown below in Figure.3:

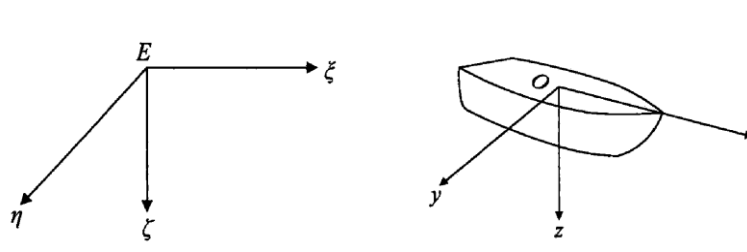


Figure.3 coordinate system[17]

The inertial coordinate $E - \zeta\eta\xi$ fixed on the ground is used to describe the actual displacement and angular displacement of the ship. The origin E can be chosen anywhere as long as it stays still. In this particular case, the origin E is fixed on the starting point, and the ζ axis is pointing at the earth's core, and the ξ -axis is pointing to the north. Considering the travel range of the personal watercrafts being relatively small, the earth curvature effect is not considered.

The Body fixed coordinate $O - xyz$ travels with the ship. The origin point O is fixed at the center of mass of the ship and x -axis points at the front and y -axis points at the starboard side.

2.4 Definition of 6-DOF (degree of freedom) motion

The motion of a sailing boat is often treated as 6-DOF. In the body-fixed coordinate $O - xyz$, naming of that behavior according to the habits is shown in figure.4 below.

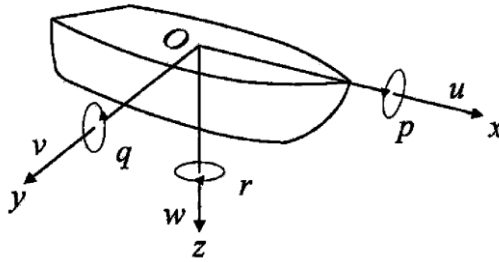


Figure.4 Motion parameters symbols in body fixed coordinate[17]

In X-axis, the translational movement surge velocity is labeled u , and the rotary movement rolling rate is labeled p . In Y-axis, the translational movement sway velocity is labeled v , and the rotary movement pitching rate is labeled q . In the Z-axis, the translational movement heave velocity is labeled w , and the rotary movement yaw rate is labeled r . Similarly, in the inertial coordinate, the heading angle, rolling angle and the pitching angle is labeled ψ, φ, θ as is shown in figure.5

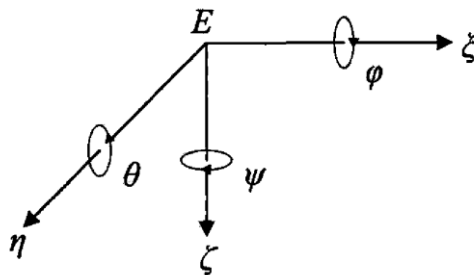


Figure.5 Motion parameters symbols in inertial coordinate[17]

2.5 Equation of translational movement

From the theorem of momentum,

The momentum of a certain object G can be expressed as follow:

$$G = \int V_p dm$$

From the theory of composition of motion:

$$V_p = V_c + \omega \times d$$

Where V_p is the velocity on any place of a rigid body, V_c is the speed at the centre of mass and ω is the angular velocity.

We have

$$G = \int (V_c + \omega \times d) dm = V_c \int dm + \omega \times \int d dm$$

Since

$$\int d dm = 0$$

Therefore

$$G = V_c \times m + 0 = mV_c$$

According to Newton's Law

$$\frac{dG}{dt} = F$$

For force vector, according to figure.6

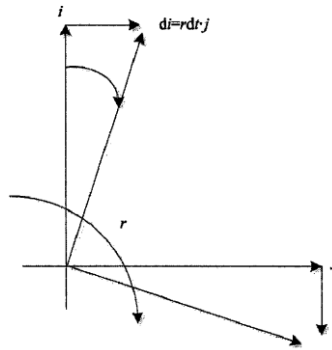


Figure.6 Unit vectors differential relationship[18]

The relationship can be determined

$$\frac{d\vec{i}}{dt} = r\vec{j}$$

$$\frac{d\vec{j}}{dt} = -r\vec{i}$$

The fundamental equation of translational movement can be determined

$$m \left(\frac{du}{dt} - vr + x_c r^2 \right) = F_x$$

$$m \left(\frac{dv}{dt} + ur + x_c \dot{r} \right) = F_y$$

The equation of motion is slightly different because the analysis is based on a body-fixed coordinate.

Generally speaking, the term $-mvr$ and mur are components of centripetal inertia forces while $-mx_c r^2$ and $mx_c \dot{r}$ are centripetal inertia forces and tangential inertia forces.

2.6 Equation of Rotary Movement

Similar to the above section, the equation of rotary movement also comes from the theorem of momentum:

$$\begin{aligned} \mathbf{H}_c &= \int (d \times V_p) dm = \int (d \times V_c) dm + \int (d \times \omega \times d) dm \\ &= \int (x_1 \mathbf{i} + y_1 \mathbf{j}) \times r \mathbf{k} \times (x_1 \mathbf{i} + y_1 \mathbf{j}) dm = r \left[\int (x_1^2 + y_1^2) dm \right] \mathbf{k} = I_{\zeta\zeta} r \mathbf{k} \end{aligned}$$

Where

$$I_{\zeta\zeta} = \int (x_1^2 + y_1^2) dm$$

Also, from the Newton's law

$$\frac{d\mathbf{H}_c}{dt} = M_c$$

Therefore,

$$I_{zz} \dot{r} + mx_c (\dot{v} + ur) = T_N$$

2.7 Forces Summary

For general case ship sailing situation, forces acting on a boat is shown below in figure.7

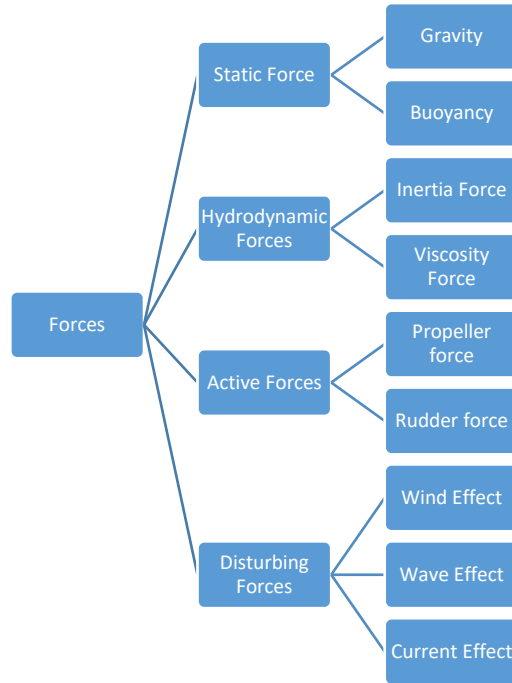


Figure.7 The force Components on a vessel

Hydrostatic forces which include gravity and buoyancy usually doesn't affect the performance of the ship. Hydrodynamic forces consist of inertia forces, which is expressed already on the left-hand side of the equation of motion, and viscosity forces[19]. Active force for general ships usually includes propeller force and rudder force. Disturbing forces usually consist of forces applied by wind effect, wave effect and current effect. Taking the hydrostatic force out of the equation, we have

$$\begin{cases} F_x = F_{xH0} + F_{xR} + F_{xP} + F_{xwind} + F_{xwave} + F_{xcurrent} \\ F_y = F_{yH0} + F_{yR} + F_{yP} + F_{ywind} + F_{ywave} + F_{ycurrent} \\ T_z = T_{zH0} + T_{zR} + T_{zP} + T_{zwave} + T_{zcurrent} + T_{zwave} \end{cases}$$

Where H0 means hydrodynamic forces, R means rudder forces and P means propelling forces. Wind, wave and current represent disturbing forces caused by wind, wave and current in each axis.

3 Mathematical Model

The Integral Hydrodynamic Model is adopted for developing the mathematical model in this paper. As is mentioned above in the literature review chapter, the idea of the Integral Hydrodynamic Model is to calculate the hydrodynamic forces by treating the hull, propeller of the impeller and the rudder as one part. Considering the fact that emphasizes are put on the ship's maneuverability, only translational movement related degrees of freedom are taken into account.

3.1 Assumptions

Before the derivation of the mathematical equations, several assumptions are needed as follows:

1. Treat the ship as a rigid body, deformations due to forces are ignored.
2. The surface of the hull is treated as a rigid boundary, which means the effect of frequency is negligible.
3. The ship is sailing on still water, wind, current and wave effects are negligible.

3.2 Factors affecting Hydrodynamics

Generally, there are 4 main factors that will affect the hydrodynamic forces applied on a boat as is mentioned in the literature review chapter. If G represents the sum of hydrodynamic forces applied on a boat, then G can become the function of the flow field characteristics, the geometry of hull, the kinematic state of the ship and the controllable inputs(rudder angle and propeller rpm) as is shown in the equation follows:

$$G = G(\text{flow characteristics, hull characteristics, kinematic state, control input})$$

In terms of flow field characteristics, it consists of physical characteristic and geometric characteristic. The physical characteristic is mainly density of seawater and the viscosity of sea water while the geometric characteristic mainly represents the depth of water, distance from shore, and the depth of immersion of the ship.

In terms of hull characteristics, it also consists of physical part and geometric part. The physical part of hull characteristics often means the friction coefficient of the surface of the hull while the geometric part of the ship simply represents the geometry of the hull, which is the main factor for determining hydrodynamic coefficients.

The kinematic state mainly represents the displacement, velocities and the accelerations in relevant degree of freedom. Unlike most of the ship whose thrusting system contains a propeller that cannot rotate and a rudder to create turning torque, the thrusting system of the REVski is shown below in figure8.



Figure.8 Outlet of the propeller duct without steering angle

When there is no steering angle, the outlet of the propeller duct is facing straight backward. In such way, all the thrusting force/power generated inside the duct by the propeller will be used to accelerate the REVski to move forward without any turning. In Figure.9 shows the outlet of the propeller duct with full right steering input, as can be seen, the outlet of the propeller rotated anti-

clockwise to generate steering torque so that rudder is required for the REVski.



Figure.8 Outlet of the propeller duct full right

So the control inputs here for the REVski are the propeller RPM(revs per minute) and the turning angle of the REVski.

3.3 Taylor expansion of the hydrodynamic function

Due to the fact that the flow field characteristic is constantly variable during the process and so are the kinematic states and the controllable inputs while the hull characteristic remains constant throughout the process, several assumptions are required below the expansion of the hydrodynamic function F .

1. The flow field characteristic remains constant in a small-time interval
2. The effect of Higher order derivatives is negligible.
3. The relationship between hydrodynamic force and acceleration is linear.
4. The hull is bilateral symmetry.
5. Force generated by the thrusting system is not taken into account in this section

Under the assumptions made above, the hydrodynamic function F :

$$F = F(u, v, r, \dot{u}, \dot{v}, \dot{r}, \delta)$$

The Taylor expansion of the function after getting rid of higher order terms:

$$F_{hydro} = F_o + F_{\dot{u}}\dot{u} + F_{\dot{v}}\dot{v} + F_{\dot{r}}\dot{r} + F_u(u - u_0) + G_v v + G_r r + G_{\delta_r} \delta_r$$

Where F_o $F_{\dot{u}}$ $F_{\dot{v}}$ $F_{\dot{r}}$ F_u G_v G_r G_{δ_r} are the hydrodynamic coefficients.

These hydrodynamic coefficients often have practical physical meanings. Generally, they represent the force acting on the axis due to the speed of acceleration. For example, the numerical value of $F_{\dot{u}}$ equals to the force acting on the axis when there is acceleration with its numerical value being \dot{u} . the 0-order term, F_o , represent the inherent hydrodynamics while all first-order represents hydrodynamics generated by speeds or accelerations [20].

3.4 Linearization of the mathematical model

Based on the hydrodynamics function above,

$$F_{hydro} = F_o + F_{\dot{u}}\dot{u} + F_{\dot{v}}\dot{v} + F_{\dot{r}}\dot{r} + F_u(u - u_0) + G_v v + G_r r + G_{\delta_r} \delta_r$$

The forces applied on each axis can be expressed as below:

$$F_x = X_o + X_{\dot{u}}\dot{u} + X_{\dot{v}}\dot{v} + X_{\dot{r}}\dot{r} + X_u(u - u_0) + X_v v + X_r r + X_{\delta_r} \delta_r$$

$$F_y = Y_o + Y_{\dot{u}}\dot{u} + Y_{\dot{v}}\dot{v} + Y_{\dot{r}}\dot{r} + Y_u(u - u_0) + Y_v v + Y_r r + Y_{\delta_r} \delta_r$$

$$T_x = N_o + N_{\dot{u}}\dot{u} + N_{\dot{v}}\dot{v} + N_{\dot{r}}\dot{r} + N_u(u - u_0) + N_v v + N_r r + N_{\delta_r} \delta_r$$

For the force of the propeller,

In x-axis:

$$F_{px} = F_{prop} \cos \alpha$$

In y-axis:

$$F_{py} = F_{prop} \sin \alpha$$

Turning torque:

$$T_{zp} = F_{p_x} d_x + F_{p_y} d_y$$

Therefore, the final expression of the force applied to each axis is

$$F_x = X_o + X_{\dot{u}}\dot{u} + X_{\dot{v}}\dot{v} + X_{\dot{r}}\dot{r} + X_u(u - u_0) + X_v v + X_r r + X_{\delta_r} \delta_r + F_{prop} \cos \alpha$$

$$F_y = Y_0 + Y_{\dot{u}}\dot{u} + Y_{\dot{v}}\dot{v} + Y_{\dot{r}}\dot{r} + Y_u(u - u_0) + Y_v v + Y_r r + Y_{\delta_r}\delta_r + F_{prop}\sin\alpha$$

$$T_z = N_0 + N_{\dot{u}}\dot{u} + N_{\dot{v}}\dot{v} + N_{\dot{r}}\dot{r} + N_u(u - u_0) + N_v v + N_r r + N_{\delta_r}\delta_r + F_{p_x}d_x + F_{p_y}d_y$$

together with the kinematic equation in the previous chapter:

$$m\left(\frac{du}{dt} - vr + x_c r^2\right) = F_x$$

$$m\left(\frac{dv}{dt} + ur + x_c \dot{r}\right) = F_y$$

$$I_{zz}\dot{r} + mx_c(\dot{v} + ur) = T_N$$

Replacing the forces with the final expression of forces applied on each axis:

In x-axis:

$$m(\dot{u} - vr + x_c r^2) = X_0 + X_{\dot{u}}\dot{u} + X_{\dot{v}}\dot{v} + X_{\dot{r}}\dot{r} + X_u(u - u_0) + X_v v + X_r r + X_{\delta_r}\delta_r + F_{prop}\cos\alpha$$

In y-axis

$$m(\dot{v} + ur + x_c \dot{r}) = Y_0 + Y_{\dot{u}}\dot{u} + Y_{\dot{v}}\dot{v} + Y_{\dot{r}}\dot{r} + Y_u(u - u_0) + Y_v v + Y_r r + Y_{\delta_r}\delta_r + F_{prop}\sin\alpha$$

In z-axis

$$I_{zz}\dot{r} + mx_c(\dot{v} + ur) = N_0 + N_{\dot{u}}\dot{u} + N_{\dot{v}}\dot{v} + N_{\dot{r}}\dot{r} + N_u(u - u_0) + N_v v + N_r r + N_{\delta_r}\delta_r + F_{p_x}d_x + F_{p_y}d_y$$

Since the hull is built to be bilateral symmetry, so for any lateral movement velocity, the relevant hydrodynamic coefficient should cancel out each other. Therefore, all relevant hydrodynamic coefficient should be zero [21]

$$X_v = 0$$

$$X_{\delta_r} = 0$$

$$X_{\dot{v}} = 0$$

$$X_{\dot{r}} = 0$$

$$Y_u = Y_{\dot{u}} = 0$$

$$N_u = N_{\dot{u}} = 0$$

In this case, after simplification, the mathematical model becomes:

$$(m - X_{\dot{u}})\dot{u} = X_u(u - u_0) + F_{prop}\cos\delta$$

$$(m - Y_{\dot{v}})\dot{v} + (mx_G - Y_{\dot{r}})\dot{r} = Y_v v + (Y_r - mu_0)r + Y_{\delta_r}\delta_r + F_{prop}\sin\delta$$

$$(mx_G - N_{\dot{v}})\dot{v} + (J_z - N_{\dot{r}})\dot{r} = N_v v + (N_r - mx_G u_0)r + N_{\delta_r}\delta_r$$

3.5 Computation of the Hydrodynamic coefficients

There are still 8 hydrodynamic coefficients needs to be determined after simplification of the mathematical model. To do so, according to Clarke. 1983, there is a linear relationship between some of the hydrodynamic coefficient and the geometry of the hull acquired by multiple ship simulations [22]:

$$Y'_{\delta} = 3.0A_R / L^2$$

$$N'_{\delta} = -(1/2)Y'_{\delta}$$

$$Y'_v = -[1 + 0.16C_b B/d - 5.1(B/L)^2] \cdot \pi(d/L)^2$$

$$Y'_r = -[0.67B/L - 0.0033(B/d)^2] \cdot \pi(d/L)^2$$

$$N'_v = -[1.1B/L - 0.041B/d] \cdot \pi(d/L)^2$$

$$N'_r = -[1/12 + 0.017C_b B/d - 0.33B/L] \cdot \pi(d/L)^2$$

$$Y'_v = -[1 + 0.40C_b B/d] \cdot \pi(d/L)^2$$

$$Y'_r = -[-1/2 + 2.2B/L - 0.080B/d] \cdot \pi(d/L)^2$$

$$N'_v = -[1/2 + 2.4d/L] \cdot \pi(d/L)^2$$

$$N'_r = -[1/4 + 0.039B/d - 0.56B/L] \cdot \pi(d/L)^2$$

In above equations, L represents the length of the ship. B represents the longest width of the ship. D represents the depth of immersion. C_b represent the block coefficients and A_R represents the thrusting effecting area [22].

3.6 Operating Response Characteristics Equation

The operating response characteristics equation is also known as second-order KT equation. Although it is not used in modeling the dynamic behavior of the REVSKI, the 2nd order KT equation

is widely used for developing the autonomous driving system of any marine vehicle [23]. This section is written as future reference if the autonomous driving function will be built on the REVski.

Based on the simplified mathematical model:

$$\begin{aligned}(m - X_{\dot{u}}) \dot{u} &= X_u(u - u_0) + F_{prop} \cos \delta \\ (m - Y_{\dot{v}}) \dot{v} + (mx_g - Y_{\dot{r}}) \dot{r} &= Y_v v + (Y_r - mu_0)r + Y_{\delta_r} \delta_r + F_{prop} \sin \delta \\ (mx_G - N_{\dot{v}}) \dot{v} + (J_z - N_{\dot{r}}) \dot{r} &= N_v v + (N_r - mx_G u_0)r + N_{\delta_r} \delta_r\end{aligned}$$

Combining the second and the third equation to get rid of v, the kinematic equation of r can be expressed as follow:

$$T_1 T_2 \dot{r} + (T_1 + T_2) \dot{r} + r = K T_3 \dot{\delta}_r + K \delta_r$$

Where T1 represent the sum of the inertial torque and T2 represent hydrodynamic torque while T3 represent torque generated by controlled inputs.

When building up the negative feedback loop for keeping the REVski to move straight, the compensate torque generated by the thrusting system is normally small compared to the moment of inertia of the REVski, So the above 2nd order KT equation can be simplified as below

$$T \dot{r} + r = K \delta_r$$

Where

$$T = T_1 + T_2 - T_3$$

The physical meaning of the above equation can be regarded as the slow turning movement of the sailing REVski under a certain inertia moment, damping moment and steering torque, which means the simplified 2nd KT equation can also be expressed as below:

$$I \dot{r} + N r = M \delta$$

Where

N represents the coefficient of the damping moment

I represent the moment of inertia of the REVski

M represents turning torque generated by the thrusting system

In this case, for the performance of the REVski in terms of a system, there are 2 key parameters

$$K = \frac{M}{N}$$
$$T = \frac{I}{N}$$

If future students are designing auto-pilot of the REVski, the above 2 values are also known as Ship control Index [23].

4 CFD simulation

4.1 Components Modeling

The SOLIDWORKS CAD software is a mechanical design automation application that lets the author sketch out the internal layout of the REVski. There are many other commercial mesh grid generators available, and the reason for choosing this one is that the author knows the SOLIDWORKS best and is currently holding a student license for using it. Based on past year student Logan Chau's project, the physical layout inside the REVski is drawn on the SOLIDWORKS software as is shown below in Figure.9.

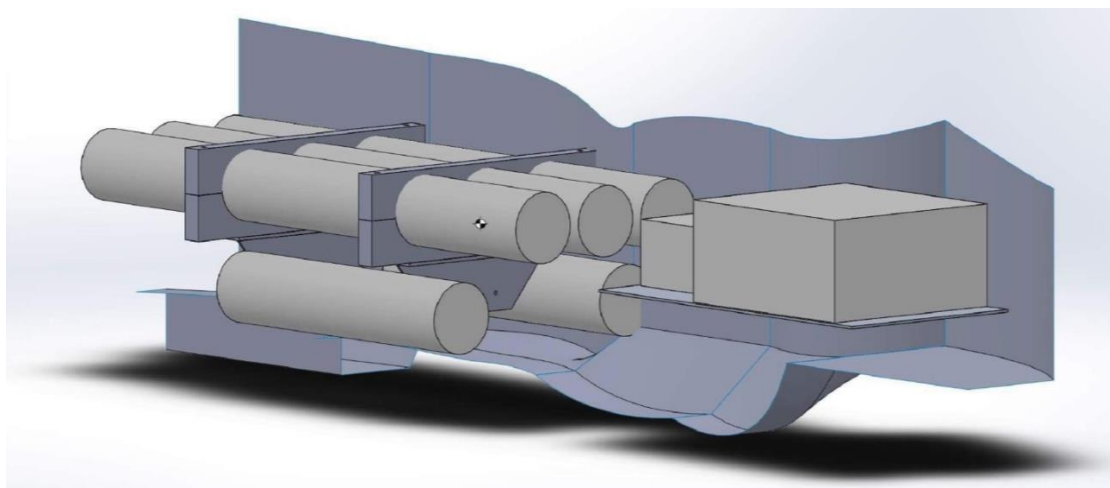


Figure.9 Mesh Grid of the internal of the REVski[25]

The above mesh grid is used to calculate the center of mass and the moment of inertia of the REVski. Components inside the REVski is taken out and measured separately as are recorded in Table.1 below

Component	Measured mass/Kg	Reference Mass/Kg	Accuracy
Motor Control Box	16.5	15.64	94.79%
Contactactor Box	4.6	4.74	97.05%
PVS Casing	83.2	83.6	99.52%
Batteries	175	174.7	99.83%
Support	80	78.1	97.63%
Total weight	359.3	356.78	99.30%

Table.1 Mass inside the REVski

The reference mass is obtained by either the manual of the individual component or from data collected from pervious student's project. As can be seen in Table.1 The accuracy of the individual component varies between 94.8% to 99.83%, which is acceptable. The mass of each component is, therefore, put into the SOLIDWORKS so that the software can return the author the center of mass and moment of inertia of the REVski.

4.2 Hull Modeling

The Hull modeling is the most important part of the CFD simulation as it directly affects the hydrodynamic coefficients. The first mesh grid of the hull is developed on SOLIDWORKS. The author measures 70 points on the left side of the hull at the front and then build up the mesh grid according to the points measured. The SOLIDWORKS mesh grid is shown below in Figure.10

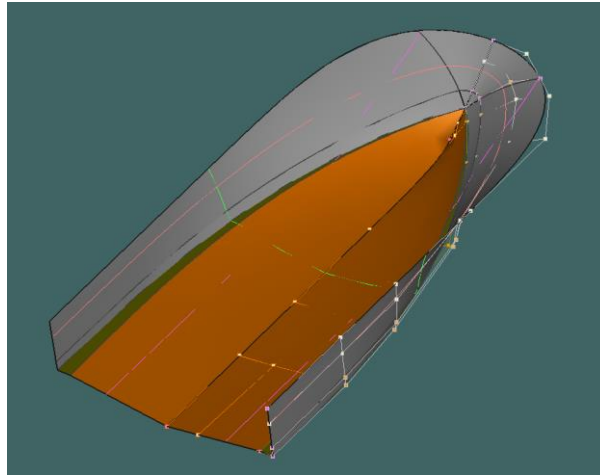


Figure.10 Mesh grid for the hull by SOLIDWORKS

However, unlike traditional mechanical modeling, the hull of the REVski consists of many complex curved surfaces, which is quite hard to accurately modeled by making sure the mesh grid passes 70 measured points. In order to eliminate errors generated in hull modeling, a more professional mesh grid generator HEXPRESS is used here to generate more accurate mesh grid. The HEXPRESS contains many in-built hull line functions for best generating the accurate hull shape. After making sure the final surface of the hull passes all 70 points, the NUBLLine (non-uniform B-shape line) function is used to create the accurate hull of the REVski. Due to the fact that the “nose” of the REVski is very hard to model and its shape affects the hydrodynamic coefficients directly, the nose of the REVski is divided and sampled individually into 6 interval, and then the fitting characteristic of these samples is chosen to be Edges Stitching function inside the HEXPRESS. On the contrary, the tail part of the REVski has a relatively little impact on the overall hydrodynamic coefficients, so some simplifications are made at the tail to minimize the workload. The Mesh Grid after HEXPRESS modifications is shown below in Figure.11

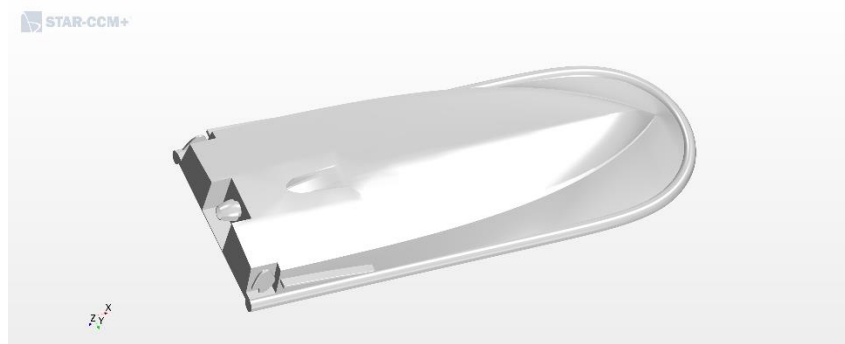


Figure.12 Mesh Grid From HEXPRESS

The weight of the hull is calculated by taking out the internal mass from the total mass of the

REVSki. The center of mass of the hull is assumed to be at the center of the geometry of the hull and the moment of inertia is obtained from the HEXPRESS assuming the same density of material throughout the hull. Combining the internal model and the hull model together in SOLIDWORKS. The final integrated mesh grid of the REVSki is shown below in Figure.13

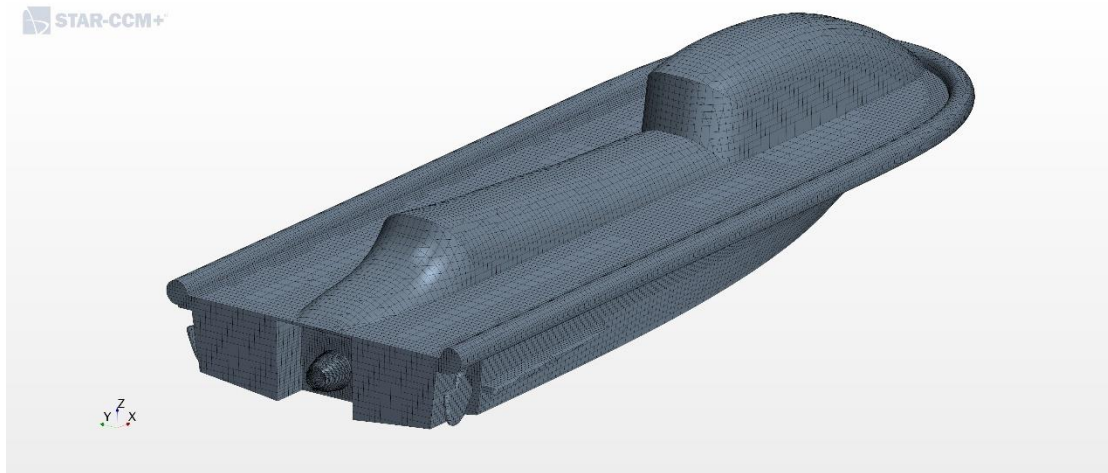


Figure.13 Integrated 3D Mesh Grid presented in STAR CCM+

4.3 Thrusting System

One of the main challenge when building up the mesh grid of the REVSki is the thrusting system since the steering system is accomplished by giving a certain angle of the outlet of the duct, unlike common ship. Based on the past student Nicholas ward's project: Effects of Torque from Electric Motors on Personal Watercraft Performance, the basic geometry parameters can be obtained as is shown in Figure.14

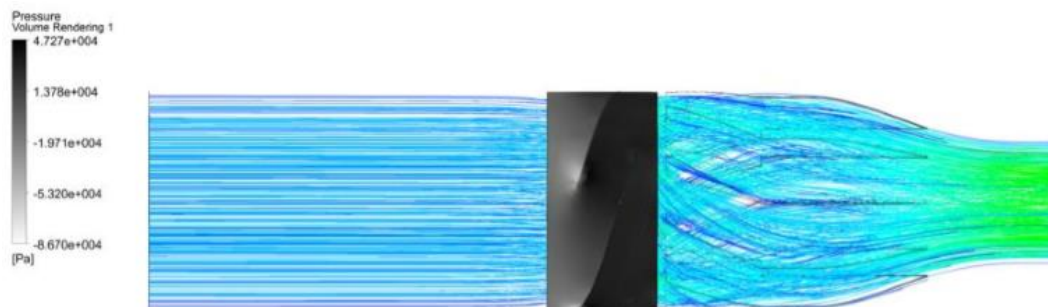


Figure.14 Normal Impeller Operation Configuration[26]

The inlet of the REVski is shown below in Figure.15



Figure.15 Inlet of the REVski

The opening area of the inlet is measured based on the real physical REVski while the shape of the inlet is slightly modified to avoid interference with other components in the mesh grid.

The outlet of the impeller duct and the steering assist side rudders as is shown in Figure.16 are modeled based on the REVski

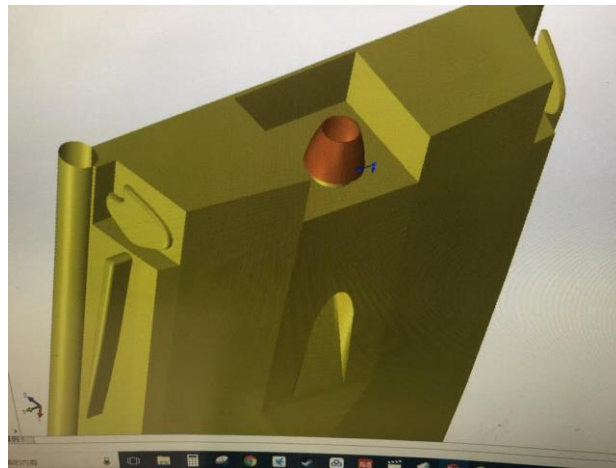


Figure.16 Outlet and Assist rudders

The impeller inside the REVski as is shown in Figure.17 is modeled based on ward's paper, and the actual shape of the impeller is slightly modified to give the same output power as is mentioned in Ward's paper

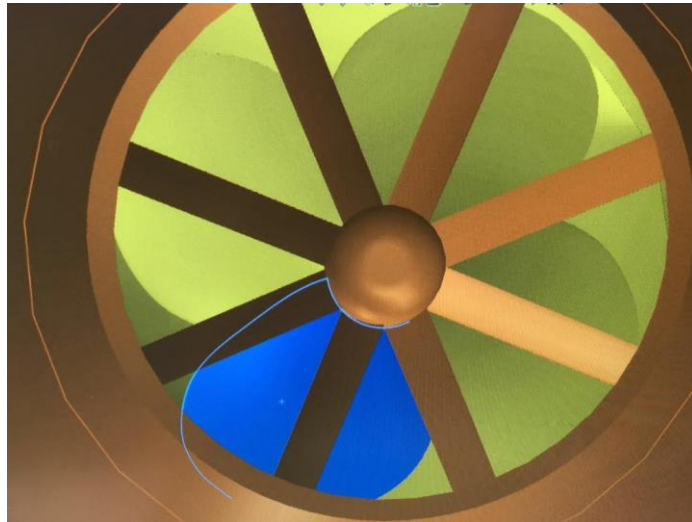


Figure.17 Propeller of the impeller

4.4 Software Setup

STAR-CCM+ is a commercial CFD software that is capable of doing marine application simulations. The paper adopts this software for carrying out CFD simulations of the REVski. Instructions for installing STAR-CCM+ can be found on Appendix.D. Apart from the accuracy of the mesh grid, the choices of flow control volume also matter with the accuracy of the final simulations. Consider the fact that the assumption of no wind and wave has already been made and the fact that bigger computational domain always leads to the more accurate result, the layout of the computation domain of the REVski is shown as follow in Figure.18:

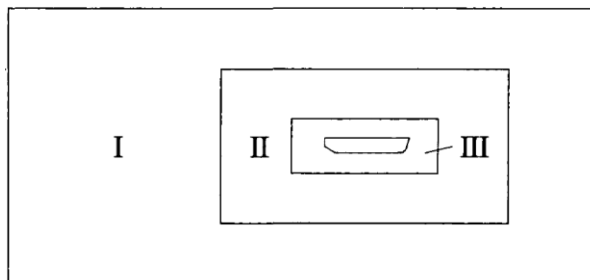


Figure.18Computation domain of the REVski

As is shown above, the whole computation domain is divided into three sub-domains. The I domain

is structured as sparse hexahedron grid as a hydrodynamic effect in this domain doesn't have much impact on the REVski. II domain centers at the center of mass of the REVski and moves along with it. II domain is defined with length and depth of 4 meters and width of 2 meters. III domain is set to be a cylinder with 1.5 meters length and 0.8 meters radius. In STARCCM+ setups, I domain is set to be stationary, II domain is set to be deforming, and III domain is set to be a rigid body.

4.5 Boundary Condition and other settings

In order to avoid the "wall" of the computation domain affecting the simulation result, the boundary condition for the computation domain around the head of the hull, and its surrounding area is set to be the velocity inlet boundary condition. The boundary condition at the tail of the REVski is set to be the pressure outlet. Turbulence intensity is set to be 5%, and the hydrodynamic radius is set to be 4 meters to avoid unreal stress concentration. The default pressure-velocity coupling index is set to be PISO. The body force weighted method is adopted for the pressure interpolation formatting. The 2nd order upwind difference method is adopted in the discrete scheme. Parallel computation is enabled for faster calculation (doesn't affect the accuracy).

4 MATLAB Simulation

The previous chapter introduced the simulation of the REVski based on the commercial software STARCCM+. As can be seen above, the simulations largely depend on the accurate mesh grid generated by SOLIDWORKS and HEXPRESS. However, Simulations for general personal watercraft cannot be accomplished by the same procedure due to the lack of the complete geometry parameters to generate accurate mesh grid. In order to carry out the simulation of the dual-jet sea-doo boat and all other small personal watercrafts, another simulation is built on MATLAB that doesn't require full geometry parameters of the object.

4.1 MATLAB flow chart

The MATLAB simulation is based on the mathematical model introduced in the previous chapter and the linear regression of the hydrodynamic coefficient. Since the linear regression of the hydrodynamic coefficient only requires 5 basic geometry parameters as input, the MATLAB simulation can predict the behavior of small personal watercraft with limited geometry information. A flow chart shown below in Figure.19 explains the basic logic of the MATLAB simulation

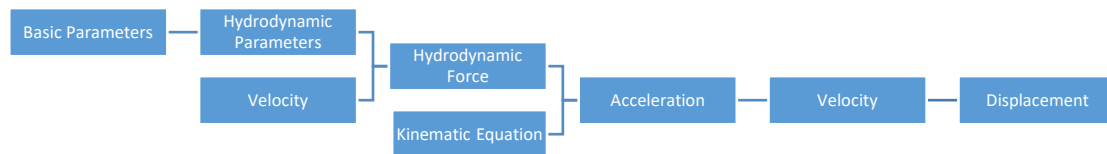


Figure.19 Flow Chart of the MATLAB Simulation

Starting from the very left, the 5 basic geometry parameters for calculating hydrodynamic coefficient (ship length, ship width, depth of immersion, block coefficient and the sectional area of the impeller duct) can be obtained or assumed much easier to the full geometry of the ship. Based on the basic parameters, the hydrodynamic coefficient is therefore calculated using the linear

regression equations as is shown below:

$$\begin{aligned}
Y'_\delta &= 3.0A_r / L^2 \\
N'_\delta &= -(1/2)Y'_\delta \\
Y'_v &= -[1 + 0.16C_b B/d - 5.1(B/L)^2] \cdot \pi(d/L)^2 \\
Y'_r &= -[0.67B/L - 0.0033(B/d)^2] \cdot \pi(d/L)^2 \\
N'_v &= -[1.1B/L - 0.041B/d] \cdot \pi(d/L)^2 \\
N'_r &= -[1/12 + 0.017C_b B/d - 0.33B/L] \cdot \pi(d/L)^2 \\
Y'_u &= -[1 + 0.40C_b B/d] \cdot \pi(d/L)^2 \\
Y'_y &= -[-1/2 + 2.2B/L - 0.080B/d] \cdot \pi(d/L)^2 \\
N'_y &= -[1/2 + 2.4d/L] \cdot \pi(d/L)^2 \\
N'_z &= -[1/4 + 0.039B/d - 0.56B/L] \cdot \pi(d/L)^2
\end{aligned}$$

Together with the velocity of the pervious time interval, the hydrodynamic forces on the current time interval can be calculated using the equations shown below:

$$F_x = X_0 + X_u \dot{u} + X_v \dot{v} + X_r \dot{r} + X_u(u - u_0) + X_v v + X_r r + X_{\delta_r} \delta_r + F_{prop} \cos \alpha$$

$$F_y = Y_0 + Y_u \dot{u} + Y_v \dot{v} + Y_r \dot{r} + Y_u(u - u_0) + Y_v v + Y_r r + Y_{\delta_r} \delta_r + F_{prop} \sin \alpha$$

$$T_z = N_0 + N_u \dot{u} + N_v \dot{v} + N_r \dot{r} + N_u(u - u_0) + N_v v + N_r r + N_{\delta_r} \delta_r + F_{p_x} d_x + F_{p_y} d_y$$

Once the forces are obtained, the kinematic equation shown below can be used to calculate the acceleration in the current time interval.

$$m \left(\frac{du}{dt} - vr + x_c r^2 \right) = F_x$$

$$m \left(\frac{dv}{dt} + ur + x_c \dot{r} \right) = F_y$$

$$I_{zz} \dot{r} + m x_c (\dot{v} + ur) = T_N$$

Based on the acceleration obtained in the previous step, by doing numerical integration, velocity and displacement of the current time interval are, therefore, obtained. These velocity and displacement information are used to calculate hydrodynamic forces in the next time interval.

4.2 SIMULINK layout

The general layout of the MATLAB model is shown below in figure.20.

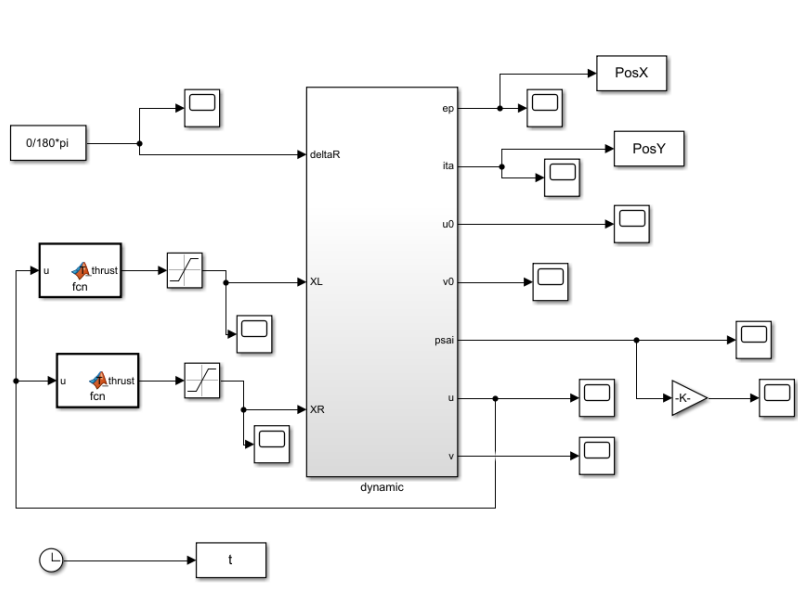


Figure.20 The layout of the SIMULINK

The dynamic model requires steering angle as the main input. Thrusting power model of the dual jet thrusting system comes from a third-party source code, which uses current heading velocity as the dynamic input. The MATLAB simulation gives trace plot and velocity diagram as output. Behind the big dynamic block in the middle is the equation of motion expressed in the Simulink flow chart way.

The SIMULINK flowchart inside the dynamic block is shown below in Figure.21. Basically, those blocks come from the equation of motion obtained in the mathematical model chapter.

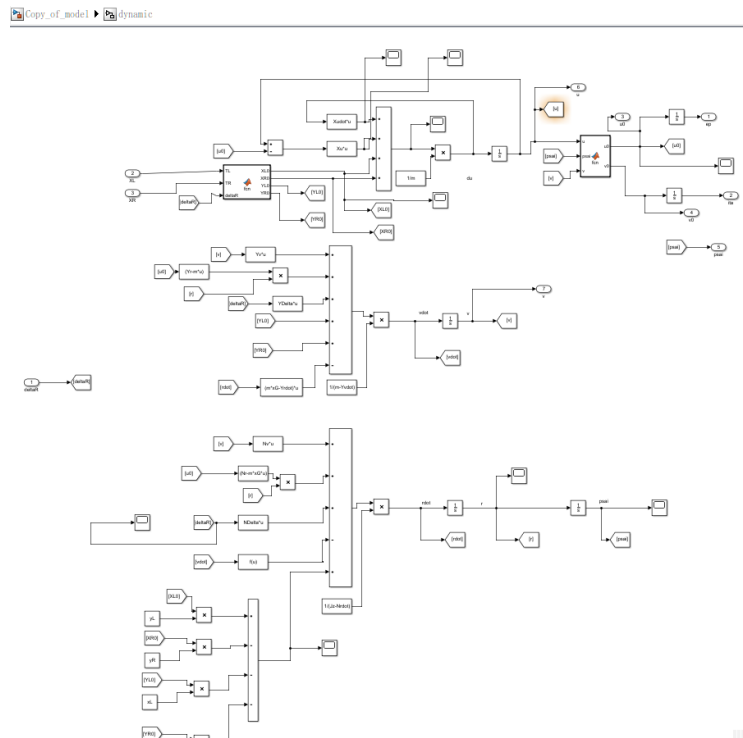


Figure.22 Simulink Flowchart inside the dynamic block

More detailed photo of the flowchart inside the dynamic block will be present in Appendix A.

4.3 Inputs for The MATLAB Simulation

As is mentioned above, the MATLAB simulation requires little geometry information for simulating the behavior of a personal watercraft. A m.file is created for all the inputs needed and calculating hydrodynamic coefficient. The full script is shown in Appendix B. Below in figure.23 is a screenshot for inputs

```

AR = 0.032;%blade area
L = 3.324;%ship total length
Cb = 0.563;%fangxing ratio
B = 1.2;%width of ship
d = 0.3;%total submerged depth/chishui/

% global YDelta NDelta Yvdot Yrdot Nvdot Nrdot Yv Yr Nv Nr m xG Jz

%10 hydrodynamic coefficients
YDelta = 3*AR/(L^2);
NDelta = -1/2*YDelta;
Yvdot = -(1+0.16*Cb*B/d - 5.1*(B/L)^2) *pi*(d/L)^2;
Yrdot = -(0.67*B/L-0.0033*(B/d)^2)*pi*(d/L)^2;
Nvdot = -(1.1*B/L-0.041*B/d)*pi*(d/L)^2;
Nrdot = -(1/12+0.017*Cb*B/d - 0.33*B/L)*pi*(d/L)^2;
Yv = -(1+0.40*Cb*B/d)*pi*(d/L)^2;
Yr = -(-1/2+2.2*B/L-0.080*B/d)*pi*(d/L)^2;
Nv = -(1/2+2.4*d/L)*pi*(d/L)^2;
Nr = -(1/4+0.039*B/d - 0.56*B/L)*pi*(d/L)^2;

Xu = 5;
Xudot = -1;
m = 530;%total weight of the ship
Jz = 5442.66;
xG = 1;
xL = xG;
xR = xG;
yL = 0.2; %distance to the middle l
yR = 0.2;

```

Figure.23 Screenshot of the datainput.m

Since the dual-jet Boat is not in the lab currently, the configuration shown above comes from the REVSKI that is currently in the lab, the author intends to run the simulation based on the REVSKI so that the result can be compared with the actual field test record and the CFD modeling record.

4.4 Setting for the solver

In order for the reader to repeat the SIMULINK simulation, the setting inside the solver should be the same as the author. The current setting shown in Figure.24 has not been optimized, and there is a possibility that different setting may result in better result.

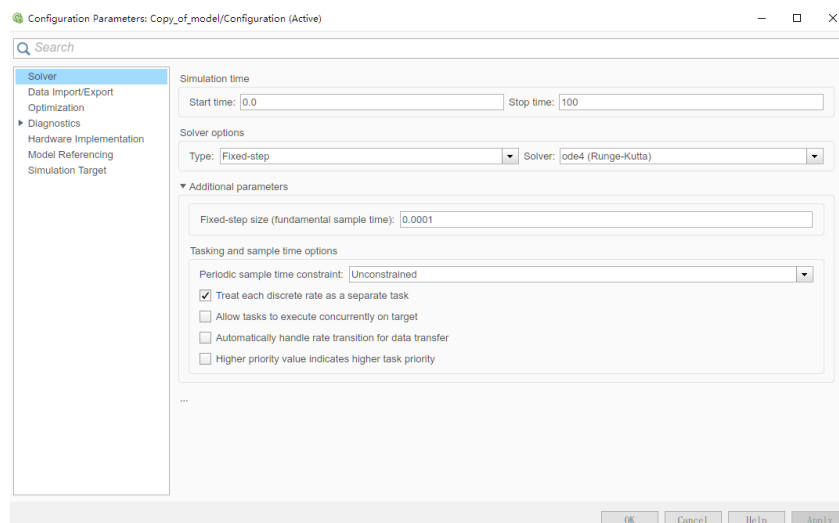


Figure.24 Configuration Parameters

5 Result and Discussion

The results from CFD modeling and the MATLAB modeling are presented in this chapter together with field test recording. However, due to the delay of the work completed, no field testing has been done after the GPS unit was implemented in the REV Ski. As a result, the trace plot from the simulations cannot be verified before the due date of the paper.

5.1 Drag acceleration simulation

The drag acceleration test is done by giving 0 steering angle and full thrust throughout the test. The field test data is recorded by the GPS unit inside a GoPro as is shown below in Figure.25. As can be seen, the top speed of the REV Ski is around 31 KPH. It is also noticed that the top speed achieved by the different driver is different. This might be caused by the different weight of different drives.



Figure.25 GoPro recording

In the CFD simulations, the Top speed frame is shown below in Figure.26. This is achieved by setting the RPM of the motor to 5000

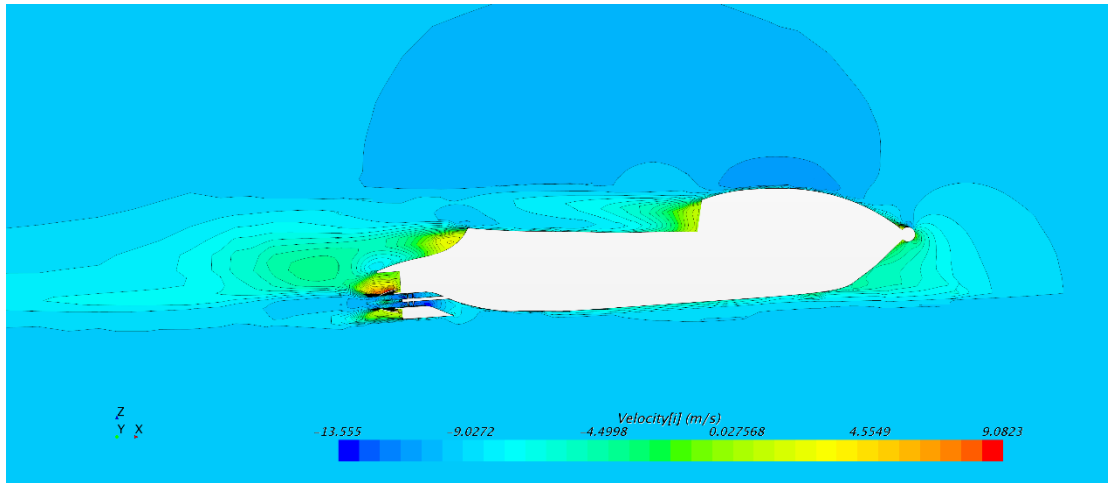


Figure.26 Top Speed at 5000 RPM

$$V_{starccm} = 9.08 \times 3.6 = 32.69 \text{ km/h}$$

It is noted that the top speed achieved by the CFD modeling is higher than the field testing result. The main reason for that is because the speed measure in the CFD modeling is the speed of the REVSki with respect to water while the top speed recorded by the GoPro is actually the ground speed. It can also be seen that the wind effect and wave effect affected on the simulation is relatively small (only around 1KPH).

Similar simulation can also be done on the MATLAB simulation. Since the origin simulation is for the dual jet boat, which will be the REV project next year, several modifications need to be done before running the drag acceleration simulation.

To let the MATLAB simulation predict the behavior of the REVSki, geometry parameters of the REVSki is needed in the datain.m. Moreover, the thrusting system needs to be changed. One of the thrusting units needs to be taken out because the REVSki only has one propeller. The flow chart after modifications are shown below in Figure.27

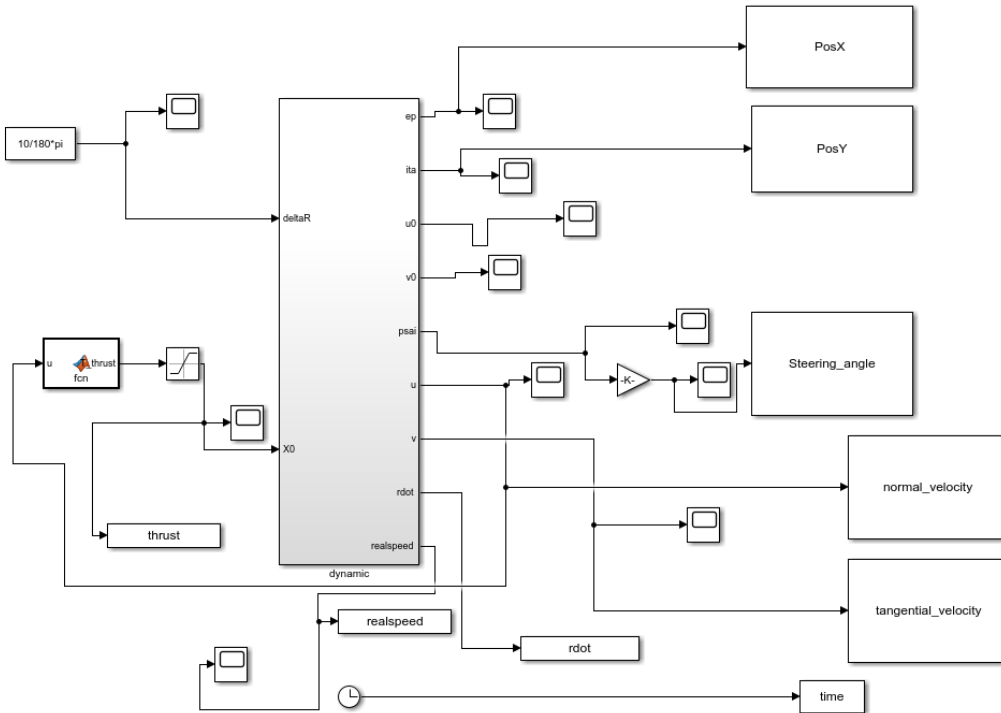


Figure.27 MATLAB Simulation for REVski

It can be seen that one of the thrusting systems is taken out and several outputs block are implemented for recording the behavior of the REVski. The final MATLAB drag acceleration simulation result is shown below in Figure.28

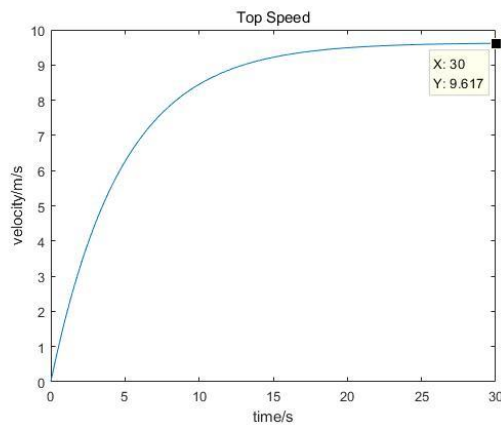


Figure.28 MATLAB Simulation result

$$V_{MATLAB} = 9.62 \times 3.6 = 34.63 \text{ km/h}$$

It can be seen that the MATLAB simulation result is a lot higher than the field testing record and the CFD modeling result. The most possible reason of that is the errors generated in the process of linear regression of the hydrodynamic coefficient because the hydrodynamic coefficient by its nature should be a variable value depends on the speed range and acceleration range while the linear

regression method fixes the hydrodynamic coefficient value throughout the whole simulation. The comparison of the calculated hydrodynamic coefficient and regression hydrodynamic coefficient will be presented later.

5.2 Bobbing Issue

According to the spread sheet of the motor, the SAE 3-phase motor installed on the REVski is capable of running at 8000 RPM. So, a CFD simulation is run on 8000RPM impeller speed. As is shown below in Figure.29

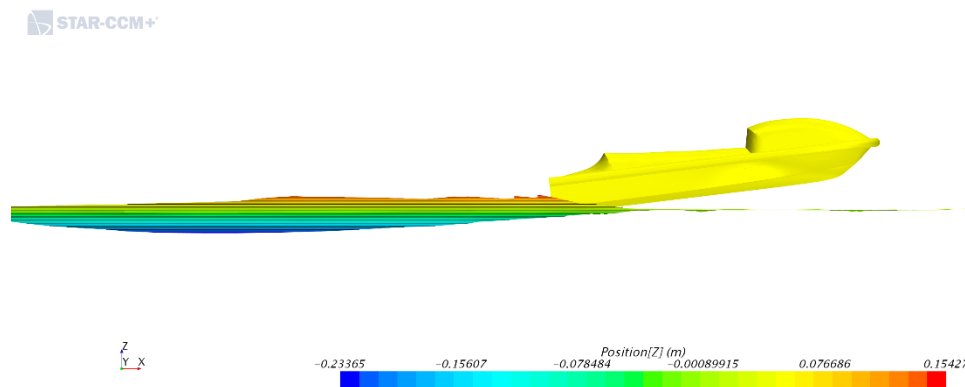


Figure.29 screenshot on 8000 RPM

It can be seen that most of the sea surface under the hull remain still while only a small area sea surface around the tail of the REVski is disturbed. This is because that the hull of the REVski is lifted because the REVski is no longer supported by the hydrostatic forces (buoyancy) but by the hydrodynamic forces components along the z-axis [24], also known as planing mode. Since hydrodynamic forces can be regarded as a function of speed, this bobbing issue is not seen when the speed is low as in the previous 32KPH simulation. The speed that occurs the bobbing issue lays around the region of 55-65 KPH. Since the STAR-CCM+ is running at marine application mode, the simulation stopped when most of the hull leaves the sea surface, so the author didn't get more detailed data for this issue. The bobbing issue itself is not bad for personal watercrafts as when this happens, the depth of immersion of the ship decreases, so the hydrodynamic forces dragging the ship decreases significantly. In such way, the object personal watercraft can achieve higher speed with smaller thrusting power. However, this put a higher requirement on the stability of the REVski

as the REVski becomes more vulnerable to disturbance such as wave and wind effect. Practically, without changing the hull shape of the REVski, the best way to do it is to lower the center of the mass by relocating the batteries on top of the motor. Alternatively, a pair of jet ski stabilizer pontoons can also do the work as is shown in Figure.30. Since the pontoons are above sea water when the Jet ski is not rolling, they will not affect the planing capability, so the performance won't be affected.



Figure.30 Jet Ski Pontoons (image from the Internet)

5.3 Comparison of Hydrodynamic Coefficients

One of the possible reasons that the simulation result from the MATLAB simulation is higher than the CFD modeling and field test is the unexpected error in the linear regression of the hydrodynamic coefficients. Since that, the hydrodynamic coefficients of the REVski is calculated using STAR-CCM+ and then compared with the linear regression results.

The purpose of introducing hydrodynamic coefficients in the first place is to describe the force applied to the object when moving on the flow field. When the speed of the object changes, according to Newton's second law, $F = ma$, the object will be applied a force in proportion to the mass and acceleration. In marine applications, this is also called associated mass. Additionally, people usually describe the drag effect of the viscosity of water by treating it as a damper. In this way, to calculate the hydrodynamic coefficient of a certain object, firstly we must record and control the force applied to the boat. Moreover, in ship maneuverability problems, first order acceleration

hydrodynamic coefficient and first-order velocity hydrodynamic coefficient is of more importance. So, in the paper, only these 2 values are calculated below.

5.3.1 Pure Transverse Drifting

Let the REVSki stay still on sea water without current and wave, apply below kinematic parameters

$$y = a \sin \omega t$$

$$\theta = \dot{\theta} = 0$$

$$v = \dot{y} = a \omega \cos \omega t$$

$$\dot{v} = -a \omega^2 \sin \omega t$$

Where

y is the lateral displacement

a is the amplitude of swing

ω is the circular frequency of the swing

θ is the angle along x-axis

In this case, the force acting on Y-axis is

$$Y = -a \omega^2 Y_v \sin \omega t + a \omega Y_v \cos \omega t + Y_0$$

And force acting on Z-axis is

$$T = -a \omega^2 N_v \sin \omega t + a \omega N_v \cos \omega t + N_0$$

The hydrodynamic coefficient can be therefore determined

$$Y_v = -\frac{F_\lambda}{a \omega^2}$$

$$Y_v = \frac{F_\mu}{a \omega}$$

$$N_v = -\frac{M_\lambda}{a \omega^2}$$

$$N_v = \frac{M_\mu}{a\omega}$$

Detailed force record is presented in Appendix C; the calculated hydrodynamic coefficient is listed below

	$Y_{\dot{v}}$	Y_v	$N_{\dot{v}}$	N_v
Computational value	0.0176398	0.045684	0.006072	0.017019
Regression Value	0.0178	0.0486	0.006	0.0183
error	0.93%	6.22%	1.20%	7.07%

Table.2 Comparison of the Hydrodynamic coefficient

It can be seen that while the error of hydrodynamic coefficient related to accelerations stays around 1% range, the errors of the speed-related hydrodynamic coefficient are about 7% lower than the computational result. This might be the reason that the top speed simulation result from the MATLAB simulation is higher than the field test record and the CFD modeling.

6 Conclusion

This paper addresses the issue of modeling the dynamic behavior of personal watercrafts. The main achievements are listed below:

1. Based on the Integral Hydrodynamic Model method, the mathematical model for describing the translational movement of the REVSKI is developed with some simplification. The equations for obtaining some of the ship control index are also developed based on the mathematical model.
2. By using the commercial CFD software STAR-CCM+, the accurate dynamic simulation for the REVSKI is built with credible simulation results
3. Based on the linear regression of the hydrodynamic coefficients found by Clarke, a MATLAB simulation is developed for any small personal watercrafts without the need for full geometry information

By comparing the results from simulations and field test data, it is found that

1. The total error in the approximation of the hydrodynamic coefficients is slightly higher than acceptable. In this case, the MATLAB simulation cannot be run for more than 30 seconds otherwise the results will be ridiculous.
2. The hull of the REVSKI is designed to trigger planing effect while the overall stability of the REVSKI may not be strong enough.
3. Cables and fuses with a higher max current allowance are required for achieving more top speed since the motor doesn't receive rated power yet.
4. The CFD modeling has greater credibility, which means the current setting for the solver inside the STAR-CCM+ is suitable for predicting the behavior of by shore personal watercrafts.

7 Future Work

If improvement of the accuracy of the modeling is required in the future, the easiest way of achieving so is to do the 3D scan of the REVski hull. Based on the experience throughout the thesis, the geometry of the hull has a direct and massive impact on the accuracy of the hydrodynamic coefficient.

If improvement of the performance of the REVski is required in the future, the first thing needs to be done to replace current fuses and cables with higher max current allowance. Similarly, the motor controller box also needs to be adjusted for allowing more current to get into the motor.

To increase the overall stability of the REVski, Rearrangement of the batteries is required since the current layout raises the center of mass of the REVski by at least 60mm. The higher center of mass for a sailing fast moving personal watercrafts will decrease the stability of the REVski. These should be done before speeding up the REVski as the REVski is very close to triggering planing phenomenon.

8 Reference

- [1] Cambridge English Dictionary. Archived from the original on 17 April 2017. Retrieved 7 May 2017.
- [2] Davidson, K. S. M., & Schiff, L. (1946). Turning and course keeping qualities of ships.
- [3] Abkowitz, M. A. (1964). Lectures on ship hydrodynamics--Steering and manoeuvrability (No. HY-5).
- [4] Abkowitz, M. A. (1980). Measurement of hydrodynamic characteristics from ship maneuvering trials by system identification (No. 10).
- [5] Inoue, K. (1990). Concept of potential area of water as an index for risk assessment in ship handling. *The Journal of Navigation*, 43(1), 1-7.
- [6] Stokes, G. G. (1880). On the theory of oscillatory waves. *Transactions of the Cambridge Philosophical Society*.
- [7] Ogawa, A., & Kasai, H. (1978). On the mathematical model of manoeuvring motion of ships. *International Shipbuilding Progress*, 25(292), 306-319.
- [8] Zhengjiang Liu, & Fengchen Wang. (1994). The Radar Plotting Method of the Effect of Course Change Inertia on Avoidance Results. 2, 9-12.
- [9] Inoue, S., Hirano, M., & Kijima, K. (1981). Hydrodynamic derivatives on ship manoeuvring. *International Shipbuilding Progress*, 28(321), 112-125.
- [10] Policastro, G., Son, D. T., & Starinets, A. O. (2002). From AdS/CFT correspondence to hydrodynamics. *Journal of High Energy Physics*, 2002(09), 043.
- [11] Gunn, D. F., Rudman, M., & Cohen, R. C. Z. (2014). Modelling Water Wave and Tethered Structure Interactions using 3D Smoothed Particle Hydrodynamics.
- [12] Sutulo, S., & Soares, C. G. (2014). An algorithm for offline identification of ship manoeuvring mathematical models from free-running tests. *Ocean engineering*, 79, 10-25.
- [13] Ursell, F. (1949). On the heaving motion of a circular cylinder on the surface of a fluid. *The Quarterly Journal of Mechanics and Applied Mathematics*, 2(2), 218-231.
- [14] Van Leeuwen, G. (1970). A simplified nonlinear model of a manoeuvring ship (No. Report 262).
- [15] Bailey, P. A. (1997). A unified mathematical model describing the maneuvering of a ship

travelling in a seaway. *Trans RINA*, 140, 131-149.

[16] Wang, Y. G., Wang, B. Q., Yang, L. M., Liu, J., Dong, X. L., & Zhou, F. H. (2016, June). Experiments and Hydrodynamic Analysis of an Adaptive Arresting Net Device for Protecting Bridge Piers Against Ship Collisions. In *ASME 2016 35th International Conference on Ocean, Offshore and Arctic Engineering* (pp. V009T12A004-V009T12A004). American Society of Mechanical Engineers.

[17] Yasukawa, H., & Yoshimura, Y. (2015). Introduction of MMG standard method for ship maneuvering predictions. *Journal of Marine Science and Technology*, 20(1), 37-52.

[18] Fluent, A. N. S. Y. S. (2011). *Ansys fluent theory guide*. ANSYS Inc., USA, 15317, 724-746.

[19] Mackie, H., Sanders, R., & Legg, S. (1999). The physical demands of Olympic yacht racing. *Journal of Science and Medicine in Sport*, 2(4), 375-388.

[20] Kallstrom, C. G., & Norrbin, N. H. (1980, June). Performance criteria for ship autopilots: An analysis of shipboard experiments. In *Ship Steering Automatic Control Symposium*.

[21] Ramaswamy, S., & Mazenko, G. F. (1982). Linear and nonlinear hydrodynamics of low-friction adsorbed systems. *Physical Review A*, 26(3), 1735.

[22] Clarke, D., Gedling, P., & Hine, G. (1983). Application of manoeuvring criteria in hull design using linear theory. *Naval Architect*, 45-68.

[23] Bech, M. I. (1972). Paper 17. Some Aspects of the Stability of Automatic Course Control of Ships. *Journal of Mechanical Engineering Science*, 14(7), 123-131.

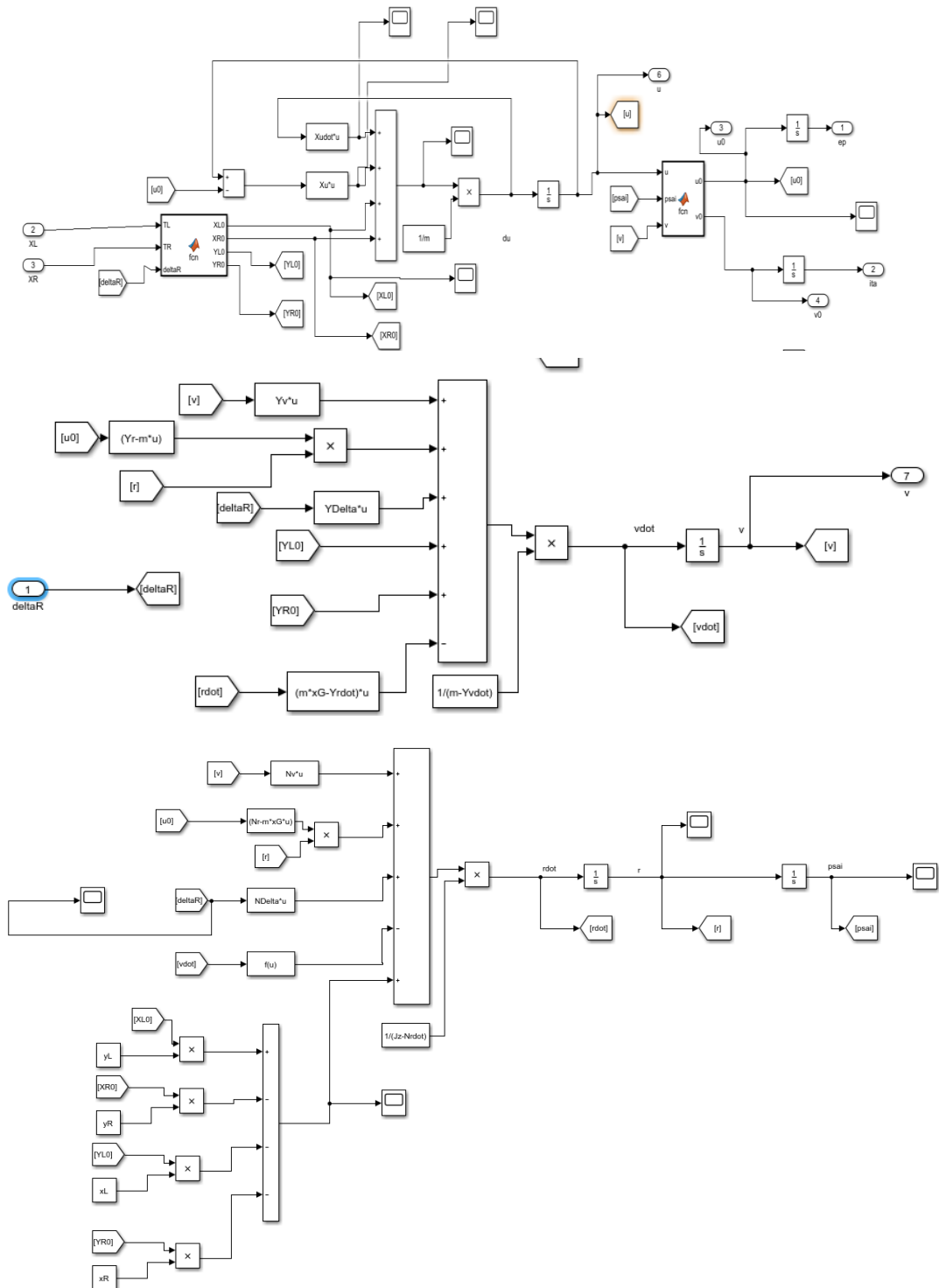
[24] Sleight, S. (2017). *The Complete Sailing Manual*. Dorling Kindersley Ltd.

[25] Chau, L. (2017) *Modelling and Design of Mounting System for An Electric Personal Watercraft*. University of Western Australia

[26] Ward, N. (2014) *Effects of Torque from Electric Motors on Personal Watercraft Performance*. University of Western Australia

9 Appendix

9.1 Appendix A-Simulink Flowchart



9.2 Appendix B-Data inputs script

```
10 AR = 0.032;%blade area
11 L = 3.324;%ship total length
12 Cb = 0.563;%fangxing ratio
13 B = 1.2;%width of ship
14 d = 0.3;%total submerged depth/chishui/
15
16 % global YDelta NDelta Yvdot Yrdot Nvdot Nrdot Yv Yr Nv Nr m xG Jz
17
18 %10 hydrodynamic coefficients
19 YDelta = 3*AR/(L^2);
20 NDelta = -1/2*YDelta;
21 Yvdot = -(1+0.16*Cb*B/d - 5.1*(B/L)^2) *pi*(d/L)^2;
22 Yrdot = -(0.67*B/L-0.0033*(B/d)^2)*pi*(d/L)^2;
23 Nvdot = -(1.1*B/L-0.041*B/d)*pi*(d/L)^2;
24 Nrdot = -(1/12+0.017*Cb*B/d - 0.33*B/L)*pi*(d/L)^2;
25 Yv = -(1+0.40*Cb*B/d)*pi*(d/L)^2;
26 Yr = -(-1/2+2.2*B/L-0.080*B/d)*pi*(d/L)^2;
27 Nv = -(1/2+2.4*d/L)*pi*(d/L)^2;
28 Nr = -(1/4+0.039*B/d - 0.56*B/L)*pi*(d/L)^2;
29
30 Xu = 5;
31 Xudot = -1;
32 m = 530;%total weight of the ship
33 Jz = 5442.66;
34 xG = 1;
35 xL = xG;
36 xR = xG;
37 yL = 0.2; %distance to the moddle l
38 yR = 0.2;
39 par = [YDelta NDelta Yvdot Yrdot Nvdot Nrdot Yv Yr Nv Nr m xG Jz];
40 psai0 = 0; % rad
41 ep0 = 0; % m
42 ita0 = 0; % m
43
44 % input
45 % deltaR = 0; %

46 save data.mat
```

9.3 Appendix C- Result from CFD Simulation

Sum of the CFD modeling Results					
Target Ground Speed	Speed at steady state	average of Drag hydrodynamic forces	impeller RPM	Propelling Force	Calculated Power
km/h	m/s	N	rpm	N.m	kW
10	2.777778	280	2206.3	12.6	2.91
30	8.333333	478	4821.4	20.1	10.15
40	11.11111	616	6646	23.8	16.56
50	13.88889	654	7205	26.08	19.68
60	16.66667	607	7510	29.69	23.35
70	19.44444	570	8050	32.5	27.40
80	22.22222	680	8550	36.1	32.32

Table.3 Sum of the key CFD Simulation Results

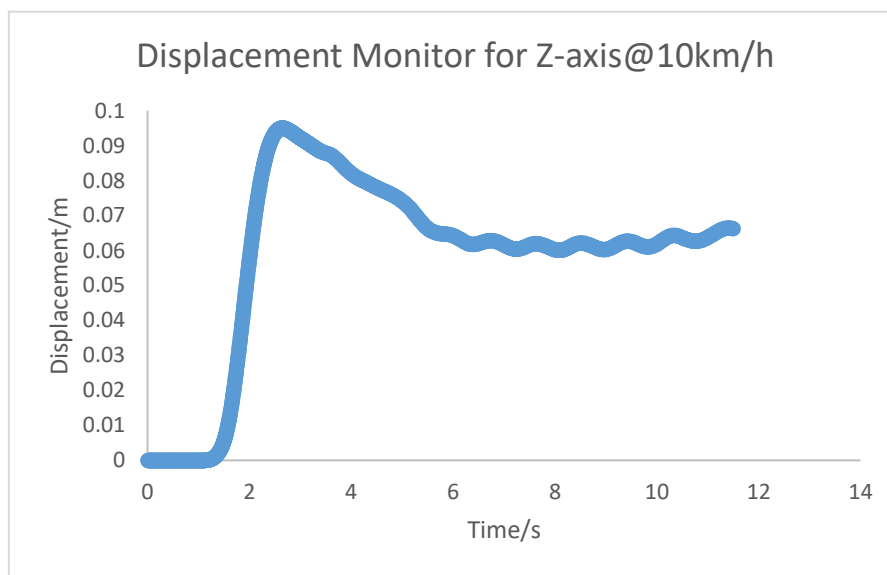


Figure.31 Displacement at Z-axis @10KM/h

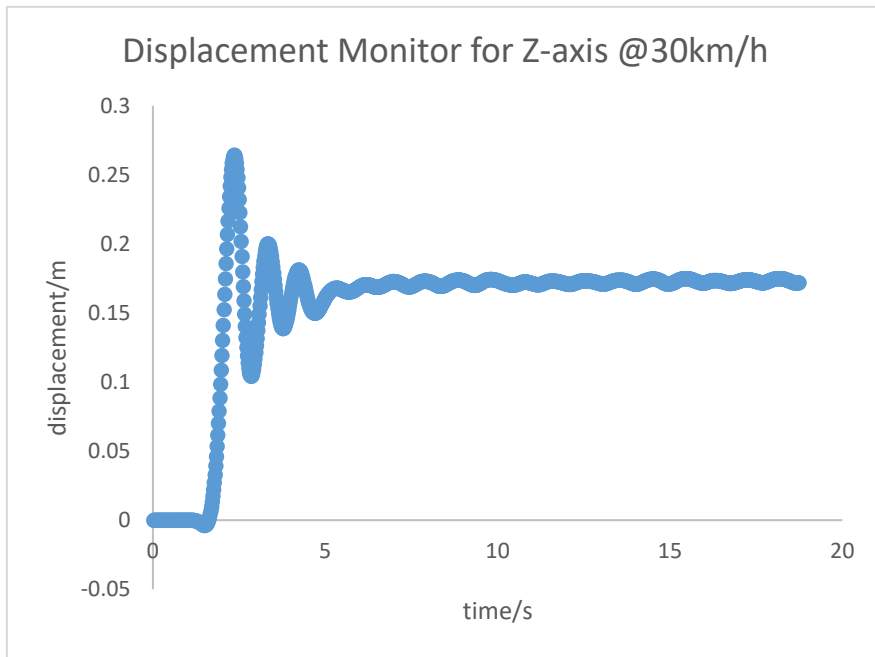


Figure.32 Displacement at Z-axis @30KM/h

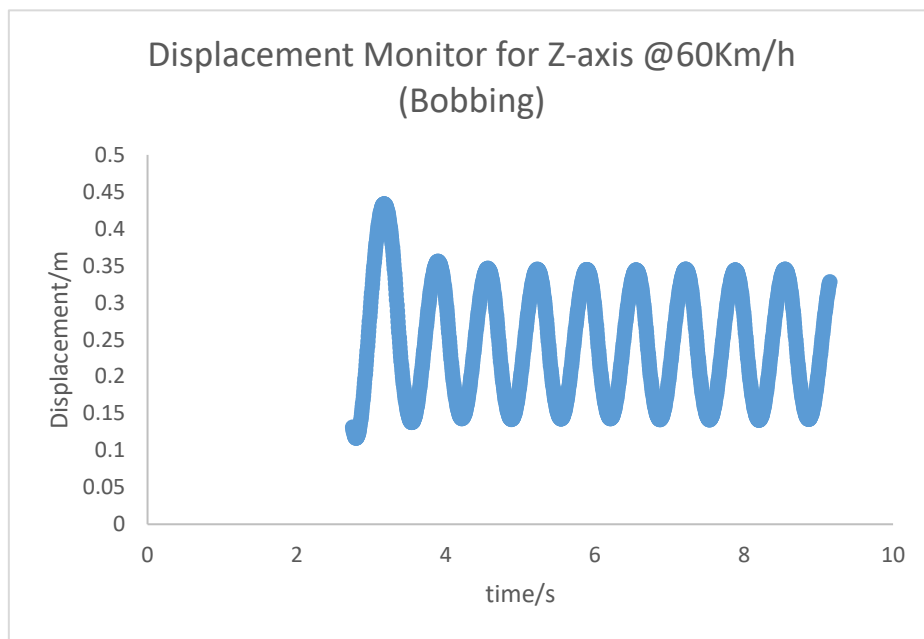


Figure.33 Displacement at Z-axis @60KM/h

9.4 Appendix D-Instruction for Installing STAR-CCM+

Download and Install Instructions for STAR-CCM+ for Windows Machines

Thank you for choosing CD-adapco for your engineering simulation requirements. A user account for our

Customer Portal "Steve" has been created for you and your username and password for this portal will

be sent to you in a separate follow up email. The Steve Portal is located at: steve.cd-adapco.com or

<http://www.cd-adapco.com/support/>

A concise description of the installation process is listed below. A description of machine requirements is

discussed in the attached HTML installation guide.

Downloading the Installation Files from the Customer Portal:

1. Go to <http://www.cd-adapco.com/support> and navigate to the Support Center link
2. Click on the link and enter your previously supplied username and password
3. Note that if this is your first visit to the support portal, you will need to change your password before continuing
4. Proceed to the File Downloads tab and click on this
5. When on the File Downloads page, select the Products Radio button
6. Ensure STAR-CCM+ appears in the selection window
7. Select the required version of the software and then choose the correct OS by clicking the appropriate 'download'
8. Download the installation guide and release notes listed in the 'Related Files and Documentation' section at the bottom of the web-page

To Install the Software:

1. Installation requires administrator privileges
2. Unzip the installation file in a temporary location
3. Navigate to the new directory named
e.g. STAR-CCM+_CadSeries7.06_win64/STARCCM+_CadSeries7.06
4. Run the executable STAR-CCM+_CadSeries7.06_win64_intel11.1.exe
5. This will display an Installation Window. For the first step License Notice, accept the license agreement and select Next
6. The next step is Choose Installation Method.
7. If this machine is the license manager:
 - a. Select Express and select Next. This will install the code in the standard location C:\Program Files\CD-adapco and install the standard components of the code.
 - b. For the Setup Licensing step, specify the path to your license and select Next. If you do not have a license file, select Next and upon completion of this installation and receipt of the license file, refer to the attached "Instructions to enable licensing on Windows"
8. If this machine is not the license manager:
 - a. Select Custom (Advanced) and select Next
 - b. At the Choose Install Type step, select Install STAR-CCM+ on this machine and select Configure Network or Local FLEXlm licensing and select Next

- c. At the Choose STAR-CCM+ Components step, select Java JDK, STAR-CCM+, STAR-View+, Microsoft VC Runtimes and select Next. Note that JAVA is not selected as one of the defaults.
 - d. For the Java Installation Directory, accept the default location and select Next
 - e. For Choose License Type, select Network and then select Next
 - f. For FlexNet client Configuration, for License Server 1 specify the port number and host name of the license server machine. The default is 1999@machine_name
 - g. For Select Install Location, accept the default location and select Next
 - h. For Additional Tasks, accept the default selections and select Next
 - i. At the Pre-Installation Summary step, review the information listed and select Install.
9. Upon completion of the installation, select Done.

To Start the Code:

1. Double click on the STAR-CCM+ icon installed on the desk top.
2. From the File Pull down menu, select New Simulation.
3. In the New Simulation window, select OK.
4. The output window will indicate if the code is able to successfully check out a license. Should the code fail to check out a license, please consult the attached "Instructions to enable licensing on Windows"

Should you encounter a licensing problem when starting the code, please send the following information to your Dedicated Application Support Engineer or support-us@cd-adapco.com:

1. The complete output including the error message
2. The value of CDLMD_LICENSE_FILE
3. The log file that written by the license manager
4. The output of Perform Status Enquiry
5. The computer/hostname and ethernet address
6. Output obtained when executing "ping hostname" from a command prompt, where hostname is the name of the license server

Further troubleshooting answers can be found in the searchable Knowledge Base in the support portal

from where the software was downloaded.